Quantum computation with classical light: The Deutsch Algorithm

Benjamin Perez-Garcia [a,c], Jason Francis [b], Melanie McLaren [c], Raul I. Hernandez-Aranda [a], Andrew Forbes [c], Thomas Konrad [b,d,∗]

[a] *Photonics and Mathematical Optics Group, Tecnológico de Monterrey, Monterrey 64849, Mexico*
[b] *School of Chemistry and Physics, University of KwaZulu-Natal, Private Bag X54001, Durban 4000, South Africa*
[c] *University of the Witwatersrand, Private Bag 3, Johannesburg 2050, South Africa*
[d] *National Institute of Theoretical Physics, Durban Node, Private Bag X54001, Durban 4000, South Africa*

ARTICLE INFO

ABSTRACT

We present an implementation of the Deutsch Algorithm using linear optical elements and laser light. We encoded two quantum bits in form of superpositions of electromagnetic fields in two degrees of freedom of the beam: its polarisation and orbital angular momentum. Our approach, based on a Sagnac interferometer, offers outstanding stability and demonstrates that optical quantum computation is possible using classical states of light.

© 2015 Published by Elsevier B.V.

1. Introduction

Quantum computation processes information encoded in quantum systems and promises unprecedented computational power by exploiting features of quantum mechanics. Since its invention three decades ago [1,2], the fascinating concept has been developed into a vibrant research field linking physics and computer science with mathematics. A variety of quantum algorithms [3] and experimental implementation techniques [4] have been explored. However, due to the difficulty of the task to coherently control and individually address a multitude of quantum systems necessary in order to improve on the speed of the best classical computers, the science community is still waiting for the first numerical result calculated by a quantum computer that is unattainable by the current conventional computer technology.

In theory it was proven already, that certain computational problems based on the use of oracles can be solved efficiently by means of quantum algorithms but not using classical ones [5]. Results in connection with period finding and the Hidden Subgroup Problem [6], for example Shor's algorithm to factorize numbers

[7,8], indicate that there are also non-oracular algorithms that can only be solved efficiently on a quantum computer.

What makes quantum computation more efficient than classical computation? Representing inputs in terms of basis states of quantum systems allows to process in parallel many inputs in form of superpositions of the basis states. However, the resulting superposition of transformed basis states representing the processed inputs would be destroyed when measured directly. Therefore, the readout of the processed information requires careful exploitation of interference effects. Moreover, entanglement is an important ingredient of quantum computation for pure states [9] but its presence is not necessary when computing with mixed states [10] as can already be seen from the first proof-of-principle implementation of the Shor Algorithm using nuclear magnetic resonance and pseudopure states without entanglement [11].

Also in classical optics the ingredients of quantum computing, as described above, i.e., superpositions, interference and indeed a form of entanglement exist. The similarities between paraxial optics and non-relativistic quantum mechanics [12] can be used to describe optics in terms of the Dirac formalism [13] and solve problems from Fourier optics elegantly using operator algebra methods from quantum mechanics [14–16]. A form of entanglement is present in classical vector beams [17–21], where the polarisation cannot be separated from the spatial dependence of the electric field [22]. This "classical" entanglement has been

* Corresponding author at: School of Chemistry and Physics, University of KwaZulu-Natal, Private Bag X54001, Durban 4000, South Africa.
E-mail address: konradt@ukzn.ac.za (T. Konrad).

used to determine the class of physically realizable Mueller matrices [23], to distinguish vector beams from scalar beams [22], and it assisted in designing schemes to realize quantum walks with classical (laser) light [24]. The recent discovery of classical entanglement has completed the list of optical ingredients which enable quantum computation.

Therefore, it is interesting to study to which extent quantum computation can be realized by means of classical optics. Here, as a first step, we apply the similarities between classical optics and quantum mechanics to demonstrate an experimental implementation of a simple quantum algorithm, the Deutsch Algorithm, with classical light. The experiment serves as a proof of principle that an oracle-based quantum algorithm can be implemented with classical light analogously to quantum systems and with the same speed-up compared to classical algorithms.

The Deutsch Algorithm can be implemented by means of different quantum systems, including cavity QED [25–27], atomic ensembles [28], quantum dots [29,30] and nuclear spins [31]. Moreover, there are several purely optical schemes which employ the polarisation and spatial modes as input and output registers for the Deutsch Algorithm. For instance, Oliveira et al. [32] used Hermite–Gaussian modes in a Mach–Zehnder interferometer to perform the algorithm, however the natural instability of the setup required additional equipment to avoid noisy results. Another approach [33] is based on a Sagnac configuration with paths qubits at the single-photon level to execute the computation. More recently, Zhang et al. suggested an implementation with a control gate conditioning the Orbital Angular Momentum (OAM) of a single photon on its polarisation state by means of a q-plate [34]. While some of these attempts already employ classical states of light (from a bright [32] and a weak laser source [33]) the authors argue that the computation is carried out by single photons many times in parallel [32] or individually [33]. Here we demonstrate using Laguerre–Gaussian (LG) beams in a stable Sagnac interferometer that classical light can be used directly to perform certain quantum computations without the need to prepare cumbersomely quantum states of light.

2. Concept and theory

There is a vast literature on quantum computation and quantum information treating in great detail the Deutsch problem [4, 35–37]. For instance, Audretsch [35] gives a good introduction. Even so, we will briefly outline the problem and its solution. Assume that a function

$$f : \{0, 1\} \to \{0, 1\} \tag{1}$$

can be accessed only via an oracle, i.e., a black box that computes the functional values $f(x)$ given the arguments x. The problem is to determine a global property of the function: whether it is constant ($f(x) = \text{const}$) or balanced (f assumes the values 0 and 1). In order to classically solve this problem, we need to query the black box at least twice. In the quantum realm, the Deutsch Algorithm allows us to determine this property in a single measurement.

f can be one of the following functions

$$
\begin{aligned}
f_1(0) &= 0, & f_1(1) &= 0, \\
f_2(0) &= 1, & f_2(1) &= 1, \\
f_3(0) &= 0, & f_3(1) &= 1, \\
f_4(0) &= 1, & f_4(1) &= 0,
\end{aligned}
\tag{2}
$$

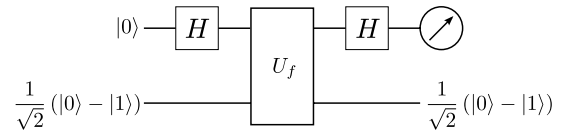where f_1 and f_2 are constant, while f_3 and f_4 are balanced functions.

Fig. 1. Quantum circuit for the Deutsch Algorithm. Here H stands for the Hadamard transformation and U_f represents the oracle. The measurement is carried out in the first register.

In order to determine the function via a quantum oracle the implementation of a unitary transformation U_f is mandatory, and its computation is done according to the rules of modular arithmetic

$$|x, y\rangle \xrightarrow{U_f} |x, y \oplus f(x)\rangle, \tag{3}$$

where $\oplus$ represents addition modulo 2 and the state vector $|x, y\rangle \equiv |x\rangle \otimes |y\rangle$ is the tensor product of the state of the first register, $|x\rangle$, with the state of the second register, $|y\rangle$. We observe that the state of the second register is dependent on the first register, in that sense U_f is said to be a controlled operation. Furthermore, the Deutsch Algorithm employs a Hadamard gate before and after the call of the quantum oracle U_f. In particular, the Hadamard gate acts on the computational basis $|0\rangle$, $|1\rangle$ as follows: $|0\rangle \xrightarrow{H} \frac{1}{\sqrt{2}}(|0\rangle + |1\rangle)$, and $|1\rangle \xrightarrow{H} \frac{1}{\sqrt{2}}(|0\rangle - |1\rangle)$.

The sequence of gates in the algorithm is described by the quantum circuit shown in Fig. 1. The required input state reads

$$|\Psi_{\text{in}}\rangle = |0\rangle \left[\frac{1}{\sqrt{2}} (|0\rangle - |1\rangle) \right]. \tag{4}$$

After the quantum circuit we obtain the state [2,38] (see Appendix A)

$$|\Psi_{\text{out}}\rangle = \left[\left((-1)^{f(0)} + (-1)^{f(1)} \right) |0\rangle + \left((-1)^{f(0)} - (-1)^{f(1)} \right) |1\rangle \right] \times \frac{1}{\sqrt{2}} (|0\rangle - |1\rangle). \tag{5}$$

From this state we can observe that if $f(0) = f(1)$ there is constructive interference on $|0\rangle$, and destructive interference on the $|1\rangle$ component for the first register. The opposite is true for $f(0) \neq f(1)$. Finally, a measurement of the computational basis in the first register reveals the answer; if we obtain a result corresponding to $|0\rangle$ the function is constant, otherwise, if we detect $|1\rangle$, the function is balanced.

To implement the algorithm we need to encode qubits in two registers. For the first register we choose the linear polarisations, horizontal and vertical, as computational basis. In the second register we use the OAM degree of freedom of LG beams to represent the computational basis states. LG beams belong to the class of helical doughnut modes (see Fig. 2) with a phase dependence of $\exp(il\theta)$, where θ is the azimuthal angle, l is known as the topological charge and carries an OAM of $l\hbar$ per photon [39–41]. The sign of l indicates the handedness of the helical (or screw-like) wavefront of the beam. A LG mode (of zero radial order) at the plane $z = 0$ may be written as [42]

$$\langle r, \theta | l \rangle \equiv \varphi_l(r, \theta) = (r/w_0)^{|l|} \exp(-r^2/w_0^2) \exp(il\theta), \tag{6}$$

where r is the radial coordinate and w_0 is the beam waist. Note that helical modes with different angular indices l, l' are orthogonal:

$$\langle l' | l \rangle = \iint\limits_{\mathbb{R}^2} \varphi_{l'}^*(r, \theta) \varphi_l(r, \theta) \, r \, dr \, d\theta = \delta_{l'l}, \tag{7}$$
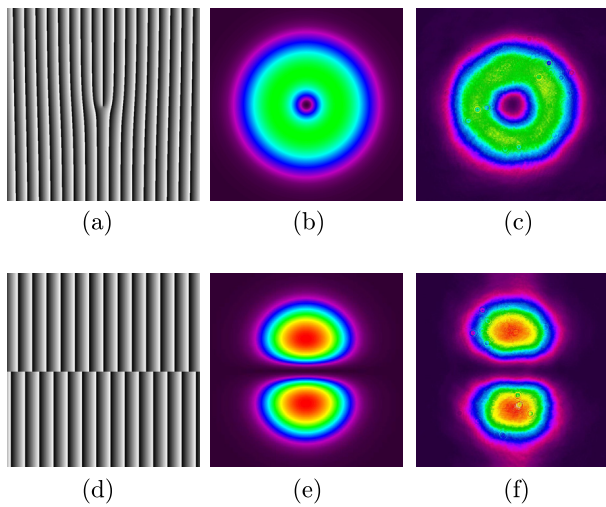
Fig. 2. The first row shows a comparison between the transversal intensity distribution of (b) the theoretical and (c) the experimental LG beam ($l = 1$). The second row shows a comparison between the intensity distribution of (e) the theoretical and (f) the experimental superposition of LG beams as given by Eq. (9) for $l = 1$. (a) and (d) display the holograms used for each case.

where $\delta_{l'l}$ is the Kronecker delta symbol. In our scheme, the basis states are represented as (see Appendix B)

$$|H, +l\rangle = |0, 0\rangle , \qquad |V, +l\rangle = |1, 0\rangle ,$$
$$|H, -l\rangle = |0, 1\rangle , \qquad |V, -l\rangle = |1, 1\rangle , \qquad (8)$$

where H and V denote horizontally and vertically polarized light respectively, and $\pm l$ stands for the handedness of the LG beam. In this scheme, the input superposition state for the Deutsch Algorithm (Eq. (4)) takes the form

$$|\Phi_{\text{in}}\rangle = |H\rangle \left(|+l\rangle - |-l\rangle\right) , \qquad (9)$$

where the second register corresponds to a superposition of helical modes.

To implement the Deutsch Algorithm, we need to emulate the action of the unitary transformation U_f of the oracle for each of the functions in Eqs. (2). This is done for each function by physically realizing the corresponding map given in Eq. (3). Thus the map U_f corresponds to one of the following quantum gates

$$
\begin{aligned}
f_1(x) &= 0, & |x, y\rangle &\xrightarrow{U_f} |x, y\rangle , \\
f_2(x) &= 1, & |x, y\rangle &\xrightarrow{U_f} |x, y \oplus 1\rangle , \\
f_3(x) &= x, & |x, y\rangle &\xrightarrow{U_f} |x, y \oplus x\rangle , \\
f_4(x) &= x \oplus 1, & |x, y\rangle &\xrightarrow{U_f} |x, y \oplus x \oplus 1\rangle .
\end{aligned}
\qquad (10)
$$

Particularly, they are given by the Identity (I), Not (NOT), Controlled-Not (CNOT) and Zero Controlled-Not (Z-CNOT) gates, respectively. The action of each quantum gate is summarized in Table 1.

Now, the task is to realize an optical implementation of these operations. The Hadamard gate is achieved by passing the input light through a half-wave plate, while the quantum gates are generated in a Sagnac interferometer by placing a dove prism, at path dependent positions. To see why this works, recall that the operation of the quantum gates are polarisation dependent; but this can be made path dependent by directing each polarisation component in its own path. Dove prisms invert the sign of the OAM [43], so by adjusting the dove prism into or out of these paths as per the requirements of the gates, the quantum circuit is realized.

Table 1
Summary of the action of quantum gates.

Input state	Identity	Not	CNOT	Z-CNOT
$|H, +l\rangle$	$|H, +l\rangle$	$|H, -l\rangle$	$|H, +l\rangle$	$|H, -l\rangle$
$|H, -l\rangle$	$|H, -l\rangle$	$|H, +l\rangle$	$|H, -l\rangle$	$|H, +l\rangle$
$|V, +l\rangle$	$|V, +l\rangle$	$|V, -l\rangle$	$|V, -l\rangle$	$|V, +l\rangle$
$|V, -l\rangle$	$|V, -l\rangle$	$|V, +l\rangle$	$|V, +l\rangle$	$|V, -l\rangle$

If the input state in Eq. (9) is passed by the quantum circuit shown in Fig. 1, the state just before the last Hadamard gate will be the following for each case:

Identity: $\quad \dfrac{1}{\sqrt{2}} \left(|H\rangle + |V\rangle\right) \left(|+l\rangle - |-l\rangle\right) ,$

NOT: $\quad -\dfrac{1}{\sqrt{2}} \left(|H\rangle + |V\rangle\right) \left(|+l\rangle - |-l\rangle\right) ,$

CNOT: $\quad \dfrac{1}{\sqrt{2}} \left(|H\rangle - |V\rangle\right) \left(|+l\rangle - |-l\rangle\right) ,$

Z-CNOT: $\quad -\dfrac{1}{\sqrt{2}} \left(|H\rangle - |V\rangle\right) \left(|+l\rangle - |-l\rangle\right) . \qquad (11)$

We observe that the resulting polarisation states in the first register are diagonal or anti-diagonal, which can be distinguished by polarimetry. For this reason, we decided to omit the last Hadamard gate. If the output beam is detected to be diagonally polarized then the function is constant, otherwise, if the output is anti-diagonally polarized, the function is balanced.

3. Experiment and results

Fig. 3 shows our experimental setup to implement the Deutsch Algorithm. In order to generate the superposition, we directed a linearly polarized HeNe laser source ($\lambda = 632.8$ nm) onto a phase-only spatial light modulator (HoloEye PLUTO VIS SLM with 1920×1080 pixels of pitch 8 μm and calibrated for a 2π phase shift at $\lambda = 632.8$ nm). After the SLM, the beam propagated through a half-wave plate (HWP) that set the polarisation of the field at 45 degrees. It then entered a Sagnac interferometer through a polarizing beam splitter (PBS), which divides the beam in two orthogonal copies. The horizontal component transmitted through the PBS moved in an anti-clockwise direction inside the interferometer, while the vertical component reflected by the PBS travelled in a clockwise sense. Both beams were eventually recombined at the same beam splitter after travelling on slightly separated trajectories in opposite directions. In order to perform the quantum gates, we used a dove prism (DP) to flip the OAM handedness of the selected component. Finally we measured the output of the interferometer with a CCD camera (Spiricon LW130). The reason for choosing a Sagnac interferometer lies in its stability properties. It is well known that amplitude division interferometers (e.g. Mach–Zehnder interferometer) need to isolate the system from the environment in order to achieve good measurements. To overcome this problem, we used a common-path interferometer in which both beams travelled the same optical path in opposite directions. As a result, the interferometer is extremely stable [44] and the relative errors of the measurement results are very small. Furthermore, our interferometer was built with three mirrors, in this sense a translation of any optical element separates the beams inside the interferometer, while maintaining aligned the output. On the other hand, a rotation in any of them, results in a tilt between both rays emerging from the interferometer.

To realize the Identity gate we added the DP altering both components. Since there was an odd number of reflections inside the interferometer we placed the DP to match the handedness of the input mode. The CNOT gate was triggered by moving the DP to
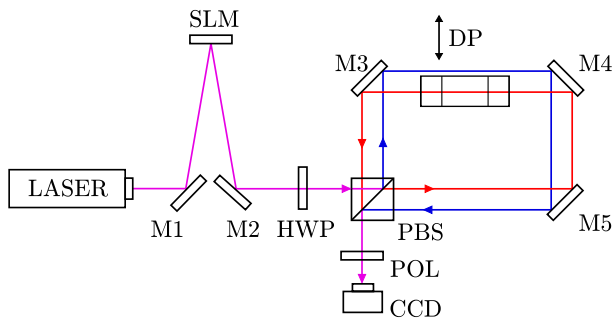
Fig. 3. Experimental implementation of the CNOT quantum gate. By moving DP we can achieve other quantum gates. (For interpretation of the references to color in this figure, the reader is referred to the web version of this article.)

modify only the horizontal component (red line in Fig. 3), while the Z-CNOT gate was performed by setting the DP to alter only the vertical component (blue line in Fig. 3). The NOT gate was generated when the dove prism was removed from the path of both components.

The measurement procedure involved varying the orientation angle of a polariser (POL) placed at the output of the interferometer. The transmission axis orientated vertically was taken to be at 0 degrees. A CCD camera was placed after the polariser and was used to gather readings of the beam intensity as the polariser angle was varied. Plotting the intensity as a function of the analyser angle allowed us to determine the polarisation state by using Malus' law. These results are shown in Fig. 4. After we measured the polarisation state of the output beam, a modal decomposition analysis was performed [45] to ensure the input and output OAM states matched for each quantum gate (see Fig. 5).

From Figs. 4(a) and 4(d) we observe that the maxima occur at 45 and 225 degrees, indicating that the output was diagonally polarized, which means in both cases, that the oracle functions were constant. On the other hand, if we look at Figs. 4(b) and 4(c) we notice that the maxima are located at 135 and 315 degrees, showing that the output was anti-diagonally polarized, which implies balanced functions of the oracle. These observations match the theoretical predictions.

4. Discussion

We proposed and experimentally verified a new method to solve the Deutsch problem using linear optical elements and classical light. The solution follows the Deutsch Algorithm and determines whether a Boolean function is constant or balanced by calling the oracle only once that computes the function values. This is half of the calls a classical computation would need.

The implementation is based on a Sagnac interferometer which guarantees the same path lengths for clockwise and counterclockwise propagating light. The resulting interferometric stability is essential for quantum computation with coherent classical light while it would be not so important when using single photon states, because they do not possess a definite phase. The implementation scheme uses superpositions of orthogonal polarisations in the first register, while the second register carries superpositions of spatial modes with different OAM values. The information thus encoded in each register corresponds to one qubit. The scheme realizes one-qubit and two-qubit gates, i.e., the Hadamard gate on the first register, the identity gate and the NOT gate on the second register as well as the controlled gates CNOT and Z-CNOT acting on the qubits in both registers.

In this way, we showed that it is in principle possible to achieve quantum computation with two qubits in the classical domain of optics. Moreover, it would be possible to implement in both registers Hadamard and phase gates which together with the CNOT gate
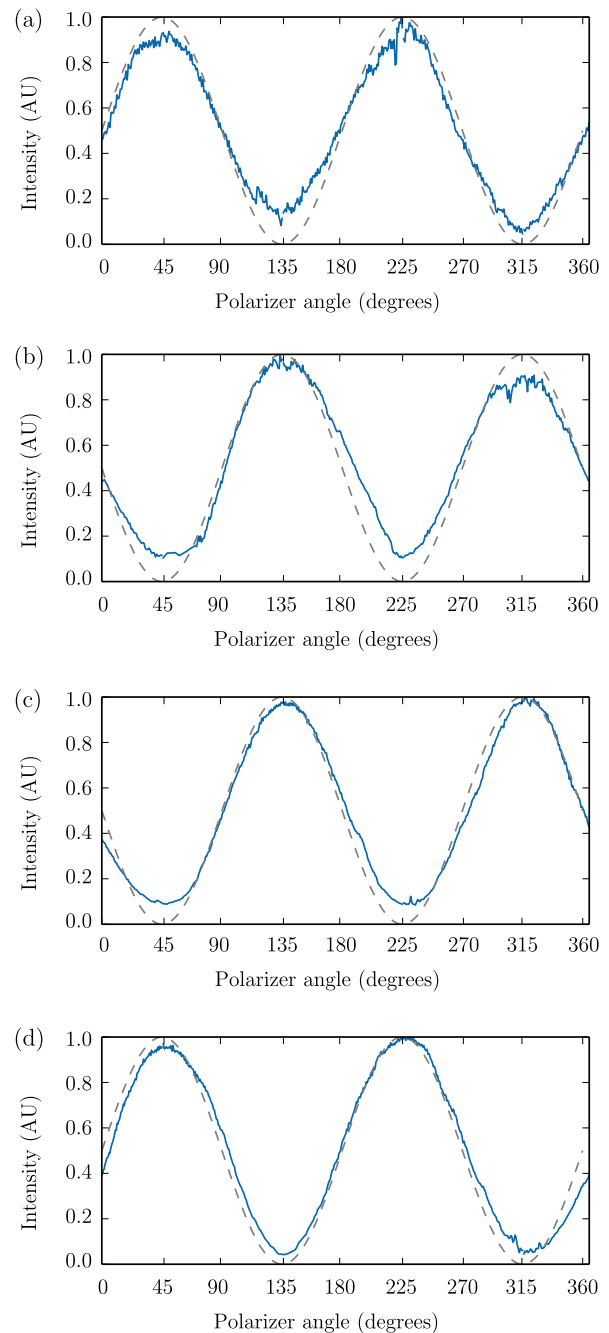

Fig. 4. Results for quantum gates. (a) Identity, (b) CNOT, (c) Z-CNOT and (d) NOT. The dotted line represents theoretical results, solid line experimental measurements.

form a set of universal quantum gates, and perform any quantum algorithm for two qubits by means of classical light and linear optics. Please note, that the scheme can in principle be operated as a genuine quantum computer by replacing the laser source, that produces a coherent state of light, by a single photon source (cp. Appendix A), provided the efficiency of the detector in the output port is sufficiently high. However, the preparation and detection of a single-photon state of light is more complex and requires more steps than that of laser light. In this sense the implementation of the quantum algorithm with classical light is more efficient than with single photons.

Here we employed two properties of the light to store two qubits. In total there are four readily accessible properties of light, i.e., the polarisation, the orbital angular momentum, the radial degree of freedom of the spatial modes and the frequency.
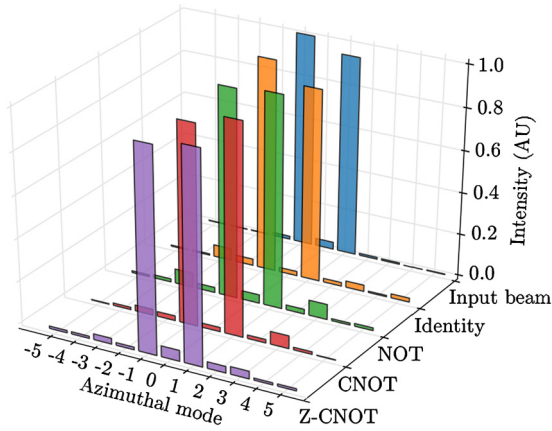
Fig. 5. Modal decomposition. We performed a modal decomposition analysis for $l \in [-5, 5]$ for the input beam and the four quantum gates.

While the polarisation corresponds to a two-dimensional Hilbert space, which prevents the scalability of our polarisation-based implementation, the remaining three properties belong to infinite-dimensional Hilbert spaces. Therefore the latter properties can in principle be used to encode an unlimited number of qubits. A way to prepare and process a large number of qubits efficiently is proposed by D. Dragoman [46]. To which extent such qubits can be used to realize other quantum algorithms is the subject of future work.

Acknowledgements

Appendix A. Description of the scheme in the Dirac formalism

In the following we describe the implementation of the Deutsch Algorithm with classical light in terms of the Dirac formalism used in quantum mechanics. This description is shown to lead to the same results as a description in the language of classical optics (cp. Appendix B). The equivalence can also be justified based on theoretical grounds [13]. Please note, that the calculations below would also describe a single photon input of the implementation scheme. In other words, the proposed scheme can be run with laser light as well as with a single photon.

The required input state is

$$|\Psi_{\text{in}}\rangle = |0\rangle \left[\frac{1}{\sqrt{2}} (|0\rangle - |1\rangle) \right], \tag{A.1}$$

where $|0\rangle$ and $|1\rangle$ represent the computational basis states. After applying the Hadamard gate to the first register we get

$$|\Psi_{\text{in}}\rangle \xrightarrow{H \otimes I} \frac{1}{\sqrt{2}} (|0\rangle + |1\rangle) \frac{1}{\sqrt{2}} (|0\rangle - |1\rangle) = |\Psi_2\rangle. \tag{A.2}$$

The unitary transformation U_f is now applied to the superposition state $|\Psi_2\rangle$ and yields

$$|\Psi_2\rangle \xrightarrow{U_f} \frac{1}{\sqrt{2}} \left((-1)^{f(0)} |0\rangle + (-1)^{f(1)} |1\rangle \right) \times$$
$$\frac{1}{\sqrt{2}} (|0\rangle - |1\rangle) = |\Psi_3\rangle. \tag{A.3}$$

After the U_f transformation, we apply another Hadamard transform in the first register to obtain the output state

$$|\Psi_3\rangle \xrightarrow{H \otimes I} \left[\left((-1)^{f(0)} + (-1)^{f(1)} \right) |0\rangle + \right.$$
$$\left. \left((-1)^{f(0)} - (-1)^{f(1)} \right) |1\rangle \right] \times \frac{1}{\sqrt{2}} (|0\rangle - |1\rangle) = |\Psi_{\text{out}}\rangle. \tag{A.4}$$

Appendix B. Description of the scheme by means of the Jones Calculus

In this appendix we calculate the state outcome of the implementation scheme using the Jones Calculus of classical optics. It turns out that this formalism yields an elegant description of the quantum computation.

By using the definition in Eq. (6) we can prepare the required superposition of modes

$$\Phi_{\text{in}} = \frac{1}{\sqrt{2}} \begin{pmatrix} \varphi_l - \varphi_{-l} \\ 0 \end{pmatrix}, \tag{B.1}$$

where the first row represents the horizontal component of the field and the second row the vertical component.

The first Hadamard transform can be achieved by passing the superposition through a half-wave plate. The matrix representation of the half-wave plate with its fast axis orientated at 22.5 degrees is

$$M_{\text{HWP}} = \frac{1}{\sqrt{2}} \begin{pmatrix} 1 & 1 \\ 1 & -1 \end{pmatrix}, \tag{B.2}$$

so

$$\Phi_2 = \frac{1}{\sqrt{2}} \begin{pmatrix} 1 & 1 \\ 1 & -1 \end{pmatrix} \frac{1}{\sqrt{2}} \begin{pmatrix} \varphi_l - \varphi_{-l} \\ 0 \end{pmatrix},$$
$$\Phi_2 = \frac{1}{2} \begin{pmatrix} \varphi_l - \varphi_{-l} \\ \varphi_l - \varphi_{-l} \end{pmatrix}. \tag{B.3}$$

The transformation U_f is now applied to the superposition Φ_2 and yields

$$\Phi_3 = \frac{1}{2} \begin{pmatrix} (-1)^{f(0)} (\varphi_l - \varphi_{-l}) \\ (-1)^{f(1)} (\varphi_l - \varphi_{-l}) \end{pmatrix}. \tag{B.4}$$

After the U_f transformation the light passes through another half-wave plate

$$\Phi_{\text{out}} = \frac{1}{2} \begin{pmatrix} ((-1)^{f(0)} + (-1)^{f(1)})(\varphi_l - \varphi_{-l}) \\ ((-1)^{f(0)} - (-1)^{f(1)})(\varphi_l - \varphi_{-l}) \end{pmatrix}, \tag{B.5}$$

which is the equivalent classical form of Eq. (A.4).

References

[1] R. Feynman, Simulating physics with computers, Int. J. Theor. Phys. 21 (1982) 467–488, http://dx.doi.org/10.1007/BF02650179.

[2] D. Deutsch, Quantum theory, the Church–Turing principle and the universal quantum computer, Proc. R. Soc. Lond. A 400 (1818) (1985) 97–117, http://dx.doi.org/10.1098/rspa.1985.0070.

[3] S. Jordan, Quantum algorithm zoo, http://math.nist.gov/quantum/zoo/ (accessed February 16, 2015).

[4] M. Nielsen, I. Chuang, Quantum Computation and Quantum Information, Cambridge University Press, Cambridge and New York, 2000.

[5] A. Berthiaume, G. Brassard, Oracle quantum computing, J. Mod. Opt. 41 (1994) 2521–2535, http://dx.doi.org/10.1080/09500349414552351.

[6] D. Boneh, J. Lipton, Quantum cryptanalysis of hidden linear functions, in: D. Coppersmith (Ed.), Crypto '95, in: Lect. Notes Comput. Sci., Springer-Verlag, 1995, pp. 424–437.

[7] P. Shor, Algorithms for quantum computation: discrete logarithms and factoring, in: Proceedings, 35th Annual Symposium on Foundations of Computer Science, 1994.

[8] P. Shor, Polynomial-time algorithms for prime factorization and discrete logarithms on a quantum computer, SIAM J. Comput. 26 (1997) 1484–1509, http://dx.doi.org/10.1137/S0097539795293172.

[9] R. Jozsa, N. Linden, On the role of entanglement in quantum computational speed-up, Proc. R. Soc. Lond. A 459 (2003) 2011–2032, http://dx.doi.org/10.1098/rspa.2002.1097.

[10] E. Bihama, G. Brassard, D. Kenigsberg, T. Mor, Quantum computing without entanglement, Theor. Comput. Sci. 320 (2004) 15–33, http://dx.doi.org/10.1016/j.tcs.2004.03.041.

[11] L. Vandersypen, M. Steffen, G. Breyta, C. Yannoni, M. Sherwood, I. Chuang, Experimental realization of Shor's quantum factoring algorithm using nuclear magnetic resonance, Nature 414 (2001) 883–887, http://dx.doi.org/10.1038/414883a.

[12] D. Gloge, D. Marcuse, Formal quantum theory of light rays, J. Opt. Soc. Am. 59 (12) (1969) 1629–1631, http://dx.doi.org/10.1364/JOSA.59.001629.

[13] S. Goyal, T. Konrad, From classical to quantum optics, in: A. Forbes (Ed.), Laser Beam Propagation: Generation and Propagation of Customized Light, CRC Press, 2014.

[14] M. Nazarathy, J. Shamir, Fourier optics described by operator algebra, J. Opt. Soc. Am. 70 (2) (1980) 150–159, http://dx.doi.org/10.1364/JOSA.70.000150.

[15] D. Stoler, Operator methods in physical optics, J. Opt. Soc. Am. 71 (1981) 334–341, http://dx.doi.org/10.1364/josa.71.000334.

[16] F. Töppel, M. Ornigotti, A. Aiello, Goos–Hänchen and Imbert–Fedorov shifts from a quantum-mechanical perspective, New J. Phys. 15 (11) (2013) 113059, http://dx.doi.org/10.1088/1367-2630/15/11/113059.

[17] R.J.C. Spreeuw, A classical analogy of entanglement, Found. Phys. 28 (3) (1998) 361–374, http://dx.doi.org/10.1023/a:1018703709245.

[18] A. Luis, Coherence, polarization, and entanglement for classical light fields, Opt. Commun. 282 (18) (2009) 3665–3670, http://dx.doi.org/10.1016/j.optcom.2009.06.024.

[19] C.V.S. Borges, M. Hor-Meyll, J.A.O. Huguenin, A.Z. Khoury, Bell-like inequality for the spin-orbit separability of a laser beam, Phys. Rev. A 82 (2010) 033833, http://dx.doi.org/10.1103/PhysRevA.82.033833.

[20] F. Töppel, A. Aiello, C. Marquardt, E. Giacobino, G. Leuchs, Classical entanglement in polarization metrology, New J. Phys. 16 (7) (2014) 073019, http://dx.doi.org/10.1088/1367-2630/16/7/073019.

[21] A. Aiello, F. Töppel, C. Marquardt, E. Giacobino, G. Leuchs, Classical entanglement: oxymoron or resource?, e-print, arXiv:1409.0213 [quant-ph], 2014.

[22] M. McLaren, T. Konrad, A. Forbes, Measuring the non-separability of classically entangled vector vortex beams, e-print, arXiv:1502.02153 [physics.optics], 2015.

[23] B.N. Simon, S. Simon, F. Gori, M. Santarsiero, R. Borghi, N. Mukunda, R. Simon, Nonquantum entanglement resolves a basic issue in polarization optics, Phys. Rev. Lett. 104 (2) (2010) 023901, http://dx.doi.org/10.1103/PhysRevLett.104.023901.

[24] S. Goyal, F. Roux, A. Forbes, T. Konrad, Implementing quantum walks using orbital angular momentum of classical light, Phys. Rev. Lett. 110 (2013) 263602, http://dx.doi.org/10.1103/PhysRevLett.110.263602.

[25] Y. Rong-Can, L. Hong-Cai, L. Xiu, C. Mei-Xiang, Implementing the Deutsch–Jozsa algorithm by using Schrödinger cat states in cavity QED, Chin. Phys. 15 (10) (2006) 2320, http://dx.doi.org/10.1088/1009-1963/15/10/021.

[26] H.-F. Wang, S. Zhang, Y.-F. Zhao, Implementing Deutsch–Jozsa algorithm with superconducting quantum interference devices in cavity QED, Int. J. Theor. Phys. 48 (2009) 2384–2389, http://dx.doi.org/10.1007/s10773-009-0028-8.

[27] S.-B. Zheng, Scheme for implementing the Deutsch–Jozsa algorithm in cavity QED, Phys. Rev. A 70 (2004) 034301, http://dx.doi.org/10.1103/PhysRevA.70.034301.

[28] S. Dasgupta, A. Biswas, G.S. Agarwal, Implementing Deutsch–Jozsa algorithm using light shifts and atomic ensembles, Phys. Rev. A 71 (2005) 012333, http://dx.doi.org/10.1103/PhysRevA.71.012333.

[29] P. Bianucci, A. Muller, C.K. Shih, Q.Q. Wang, Q.K. Xue, C. Piermarocchi, Experimental realization of the one qubit Deutsch–Jozsa algorithm in a quantum dot, Phys. Rev. B 69 (2004) 161303, http://dx.doi.org/10.1103/PhysRevB.69.161303.

[30] M. Scholz, T. Aichele, S. Ramelow, O. Benson, Deutsch–Jozsa algorithm using triggered single photons from a single quantum dot, Phys. Rev. Lett. 96 (2006) 180501, http://dx.doi.org/10.1103/PhysRevLett.96.180501.

[31] F. Shi, X. Rong, N. Xu, Y. Wang, J. Wu, B. Chong, X. Peng, J. Kniepert, R.-S. Schoenfeld, W. Harneit, M. Feng, J. Du, Room-temperature implementation of the Deutsch–Jozsa algorithm with a single electronic spin in diamond, Phys. Rev. Lett. 105 (2010) 040504, http://dx.doi.org/10.1103/PhysRevLett.105.040504.

[32] A.N. de Oliveira, S.P. Walborn, C.H. Monken, Implementing the Deutsch algorithm with polarization and transverse spatial modes, J. Opt. B, Quantum Semiclass. Opt. 7 (9) (2005) 288, http://dx.doi.org/10.1088/1464-4266/7/9/009.

[33] P. Zhang, R.-F. Liu, Y.-F. Huang, H. Gao, F.-L. Li, Demonstration of Deutsch's algorithm on a stable linear optical quantum computer, Phys. Rev. A 82 (2010) 064302, http://dx.doi.org/10.1103/PhysRevA.82.064302.

[34] P. Zhang, Y. Jiang, R.-F. Liu, H. Gao, H.-R. Li, F.-L. Li, Implementing the Deutsch's algorithm with spin-orbital angular momentum of photon without interferometer, Opt. Commun. 285 (5) (2012) 838–841, http://dx.doi.org/10.1016/j.optcom.2011.11.024.

[35] J. Audretsch, Entangled Systems: New Directions in Quantum Physics, Wiley, 2008.

[36] L. Diosi, A Short Course in Quantum Information Theory: An Approach from Theoretical Physics, Lect. Notes Phys., Springer, 2011.

[37] J. Stolze, D. Suter, Quantum Computing: A Short Course from Theory to Experiment, Wiley, 2008.

[38] D. Deutsch, R. Jozsa, Rapid solution of problems by quantum computation, Proc. R. Soc. Lond. A 439 (1907) (1992) 553–558.

[39] L. Allen, M.W. Beijersbergen, R.J.C. Spreeuw, J.P. Woerdman, Orbital angular momentum of light and the transformation of Laguerre–Gaussian laser modes, Phys. Rev. A 45 (1992) 8185–8189, http://dx.doi.org/10.1103/PhysRevA.45.8185.

[40] M.V. Berry, Paraxial beams of spinning light, Proc. SPIE 3487 (1998) 6–11, http://dx.doi.org/10.1117/12.317704.

[41] A.M. Yao, M.J. Padgett, Orbital angular momentum: origins, behavior and applications, Adv. Opt. Photonics 3 (2) (2011) 161–204, http://dx.doi.org/10.1364/AOP.3.000161.

[42] L. Allen, M. Padgett, M. Babiker, {IV} The Orbital Angular Momentum of Light, Prog. Opt., vol. 39, Elsevier, 1999, pp. 291–372.

[43] N. González, G. Molina-Terriza, J.P. Torres, How a Dove prism transforms the orbital angular momentum of a light beam, Opt. Express 14 (20) (2006) 9093–9102, http://dx.doi.org/10.1364/OE.14.009093.

[44] P. Hariharan, Optical Interferometry, Electronics & Electrical, Academic Press, 2003.

[45] I.A. Litvin, A. Dudley, F.S. Roux, A. Forbes, Azimuthal decomposition with digital holograms, Opt. Express 20 (10) (2012) 10996–11004, http://dx.doi.org/10.1364/OE.20.010996.

[46] D. Dragoman, *n*-step optical simulation of the *n*-qubit state: applications in optical computing, Optik 113 (10) (2002) 425–428, http://dx.doi.org/10.1078/s0030-4026(04)70193-x.